Thin Solid Films 562 (2014) 218–222

Contents lists available at ScienceDirect

Thin Solid Films

journal homepage: www.elsevier.com/locate/tsf

Study on target–film structural correlation in thin cobalt ferrite films grown by pulsed laser deposition technique

V. Bilovol *, L.G. Pampillo, F.D. Saccone

Laboratorio de Sólidos Amorfos, INTECIN-CONICET, Facultad de Ingeniería, Universidad de Buenos Aires, Buenos Aires C1063ACV, Argentina

ARTICLE INFO

Article history:
Received 1 August 2013
Received in revised form 14 April 2014
Accepted 15 April 2014
Available online 24 April 2014

Keywords:
Cobalt ferrite
Thin films
Pulsed laser deposition
Structural properties
X-ray absorption near edge structure

ABSTRACT

We prepared three films of crystalline cobalt ferrite under identical deposition conditions (time, temperature, pressure) using three different targets consolidated from $CoFe_2O_4$ (CFO) crystalline nanoparticles (NPs). The NPs were previously prepared by a chemical route varying their synthesis conditions in order to promote different variations in the degree of structural distortions. The purpose of this work is to study how the degree of crystal distortion of the precursor material (target) influences the structural properties of the films when they are grown by pulsed laser deposition (PLD). ^{57}Fe Mössbauer spectroscopy was used to study the local environment of iron atoms in the powders (targets for PLD). The Williamson–Hall plots were used to show the degree of the strain present in the films. X-ray absorption near edge structure spectra of the films, taken in grazing incidence geometry, were also carried out. The results explicitly demonstrate that the film with the largest strain was deposited using structurally more imperfect CFO powders whereas the film with the smallest strain was grown using the best powder from the structural point of view. These results were reinforced indirectly by magnetic measurements (exchange bias effect) in Fe/CFO bilayers (thin iron film was deposited additionally for this purpose) when hysteresis loops were analyzed after field cooling at a 3 T magnetic field. We show that the quality of thin cobalt ferrite films depends on the quality of the precursor material when the PLD technique is involved.

1. Introduction

It is known that the quality of the target strongly influences the film properties. Studies on structural relation between the target and the grown films are very important to fabricate controllable-properties of thin films. Cobalt ferrite (CFO) films have attracted considerable scientific interest because of their exceptional properties such as high coercivity and permeability at high frequencies, high chemical and mechanical stability for industrial purposes and also relatively low conductivity [1,2]. Pulsed laser deposition (PLD) growth is one of the widely used methods for CFO films' deposition because, as it is well known, this technique has the capacity to reproduce the target composition with relative facility and precise control of stoichiometry [3,4].

While a large number of reported works on CFO films are devoted to study the relationship between the deposition conditions (temperature, time, atmosphere, substrate and so on) [5–9] and film properties, little attention has been paid to the study of the structural relationship between the target and the film. In some previous works the authors analyzed the cation distribution on the magnetic properties of $ZnFe_2O_4$ and $CuFe_2O_4$ magnetic thin films grown by PLD [10,11].

In this work, we focused our attention on the pair target–film and their structural correlation. Knowing well this relationship, it could help tuning the magnetic properties of films when particular features are required. Such may be the case, for instance, of the exchange bias (EB) effect that has become an integral part of spintronics with implications for basic research and for numerous device applications like random access magnetic storage units and spin valves. ^{57}Fe Mössbauer effect spectroscopy (ME), X-ray diffraction (XRD), X-ray absorption near edge structure (XANES) technique and magnetic measurements were involved to demonstrate the relationship between the target quality and the fabricated films. Particularly, the XANES technique, a powerful synchrotron radiation tool, was applied in the grazing incidence geometry near the critical angle for total reflection where the X-ray beam is confined within a few nanometers of the surface, for studying the local distortions of probe atom.

2. Experimental details

Iron(III) nitride nanohydride ($Fe(NO_3)_3.H_2O$, 99%, Anedra) and cobalt(II) chloride hexahydride ($CoCl_2.6H_2O$, 98%, Cicarelli) were used to synthesize $CoFe_2O_4$ nanoparticles by co-precipitation method in a NaOH medium, keeping the molar ratio of Co/Fe = 0.5. Each ingredient was dissolved in a NaOH solution and then the solutions were mixed. The digestion was performed at 80 °C for 120 min. After the digestion,

* Corresponding author.
E-mail address: vbilovol@fi.uba.ar (V. Bilovol).

http://dx.doi.org/10.1016/j.tsf.2014.04.060
0040-6090/

the gelatinous precipitate was filtered and washed several times using deionized water until the pH value of the solution became neutral. Finally, the gelatinous precipitate was dried at room temperature in air to obtain a powder sample.

The nanoparticles of $CoFe_2O_4$, with mean crystallite size $d \approx 5$ nm, from the same batch were divided into three portions to be annealed at different conditions to promote variations on the structural features. One third was thermally annealed (TA) at 700 °C for 5 h. After standard pressing (1.4 GPa), the corresponding target was labeled as *cfo1*. A second portion was thermally treated at 1000 °C for 5 h, with the target label being *cfo2*. For the *cfo1* target, using the XRD technique and grain size refinement by the Debye–Scherrer formulae, d was determined as 36 nm, while for the *cfo2* target, $d \approx 49$ nm. In order to elucidate any dependence of the crystallite size on the results, we worked with a third target, *cfo3*, that was obtained by the following steps: i) TA at 1000 °C × 5 h ($d \approx 49$ nm), ii) ball milling (2 h), and iii) TA at 1050 °C × 5 h ($d \approx 36$ nm). The density of the targets is approximately 3400 kg/m^3.

Films of $CoFe_2O_4$ were deposited on Si (111) substrates by PLD using a Nd:YAG (Quanta Ray) laser at a wavelength of 355 nm, a repetition rate of 10 Hz and a fluence of 2 J/cm^2. The pressure in the chamber during the deposition was 4 Pa with a substrate temperature of 600 °C. Deposition time was 10 min with an average deposition rate of about 4 nm min^{-1}. Structural properties were analyzed by XRD in a θ–2θ diffractometer (Rigaku D/max equipped with a vertical goniometer) using Cu-K_α radiation and by ME under transmission geometry at room temperature (RT) with a standard constant acceleration spectrometer using a 10 mCi ^{57}CoRh radioactive source. The isomer shifts (δ) were referred to α-Fe. The magnetic properties were investigated (at RT and 20 K) in a Quantum Design PPMS vibrating sample magnetometer. Grazing incidence X-ray fluorescence (GIXRF) measurements were carried out at the XRF Fluorescence beamline of the LNLS (Campinas, Brazil), using a monochromatic X-ray beam of 9.7 keV. The setup includes 150-μm-vertical and 4-mm slits limiting the beam size on the sample mounted on a high-precision goniometer. Angular scans around the critical angle of total (external) reflection were performed (between 0 and 2°). The fluorescence emissions were collected using a 15-element Ge detector. After the angular scan, XANES Fe K edge (7112 eV) spectra in fluorescence mode were collected at different grazing angles using a Si (111) channel-cut monochromator. The incident beam intensity and the energy calibration were monitored using an ion-chamber and a Fe metal standard.

For the films' labels, we adopted capital letters coinciding with the corresponding targets (for instance, the CFO1 film was deposited using the *cfo1* target).

3. Results and discussion

XRD data of the cobalt ferrite films are shown in Fig. 1. At low angles, the amorphous signal of the sample-holder contributes to the diffraction pattern together with the peak of the Si substrate. As it can be seen, all films have a preferential <111> orientation. It was found that the value of the lattice constant a of the cobalt ferrite deviates from its bulk value 8.38 Å [12]. In all three samples using the position of (222) Bragg peak, the obtained a value is lower (in the range of 8.33 to 8.37 Å). This indicates that the crystallites of the films are under some strain. Fingerprints of the (311) peak, the most intense in polycrystalline cobalt ferrite, are also present, indicating that the films are not epitaxial.

Short range order in the iron probes of the powder employed for target consolidation was analyzed by ^{57}Fe ME. As this technique is sensitive to the iron environment, its spectral hyperfine parameters can give us valuable information about distortion of the crystalline lattice and bond properties. Bulk cobalt ferrite has an inverse spinel structure with one half of Fe 3+ ions on tetrahedral (A) sites and the other half together with Co 2+ ions on octahedral (B) sites [13].

We used two subspectra (sextets, corresponding to the Zeeman magnetic splitting of energy levels of the nucleus) for fitting procedures using Lorentzian shape lines. By similarity, only one fitted spectrum is shown (Fig. 2). The fitting parameters are collected in Table 1. One sextet corresponds to Fe^{3+} on the A sites, the other to Fe^{3+} on the B sites. The values of hyperfine magnetic fields as well as the values of the isomer shifts for both sites are very similar to those reported for partially inverted cobalt ferrite [12]. In the case of the *cfo2* target, the value of the quadrupole shift, 2ε, is zero for both sites, indicating that iron ions have a cubic symmetry.

For the *cfo3* target ($d \approx 36$ nm) δ, corresponding to Fe in the octahedral geometry, is a little higher (0.39 mm/s) than the observed for the *cfo2* target. Isomer shift brings out information about charge density (at nuclear sites), which can be modified by varying Fe–O bond length. The increase of δ is attributed to the change in the $Fe^{3+}-O^{2-}$ distance at the octahedral sites due to crystal distortion. When the distance of the ligand oxygen to iron is larger in the oxygen polyhedral, the lower is the *s*-electron density (at the Fe-nucleus), which results in increasing of the isomer shift. On the other hand, it was found that the quadrupole shift is distinct from zero, which indicates a deviation of iron's environment from cubic symmetry. This fact is related to synthesis conditions of the target powder. Since for the *cfo1* target ($d \approx 36$ nm), the δ value is even higher (0.41 mm/s), the deviation from cubic symmetry is more significant ($2\varepsilon = -0.07$ mm/s) suggesting even higher distortion of oxygen polyhedral.

Taking into account the sextet areas, proportional to the iron population in each site, we estimated that the concentration of Co^{2+} ions on the B-sites is the lowest in the *cfo1* target (about 46%). This means that Fe^{3+} ions occupying the B-sites (octahedral) are surrounded not only by Fe^{3+} ions on the A-sites, but also by some Co^{2+} ions on the A-sites (neither δ nor 2ε, for Fe in this latter position varies significantly for all powders, indicating that octahedral sites are more sensitive to structural distortion). Then, by this way it can be explained the existence of more distorted environments for Fe ions on the B-sites for the *cfo1* powder

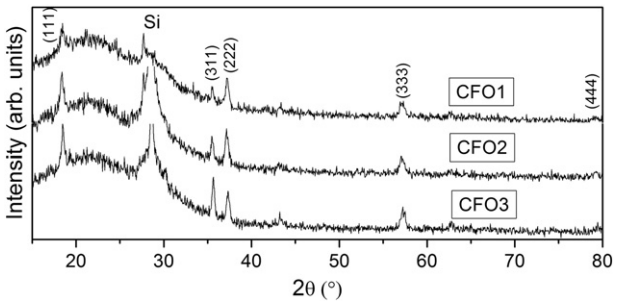

Fig. 1. XRD patterns of the films.

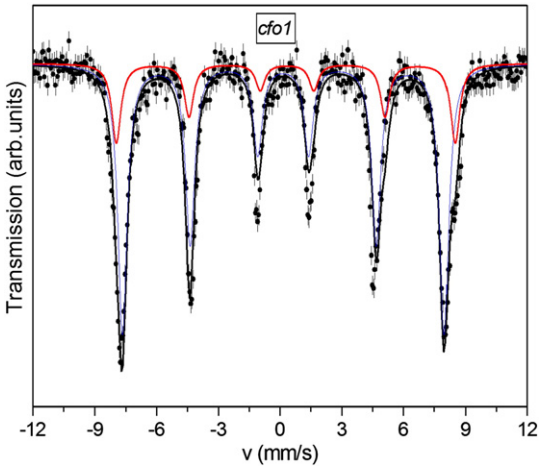

Fig. 2. Mössbauer spectrum of the target *cfo1*.

Table 1
Mössbauer fitted parameters of the targets. Errors in the isomer shift (δ), quadrupole shift (2ε), and linewidth (Γ) are less than 0.01 mm/s. Uncertainty in the hyperfine field value (B_{hyp}) and area is about 0.02 T and 5%, respectively. A—tetrahedral site, B—octahedral site. S^* is the strain value of the films from corresponding targets (CFO) using W—H plots.

Target	B_{hyp} (T)		δ (mm/s)		2ε (mm/s)		Area (%)		Γ (mm/s)	S^*, $\times 10^{-3}$
	A	B	A	B	A	B	A	B		
cfo3	49.3	52.2	0.26	0.39	0	-0.04	30.7	69.3	0.49	1.50
cfo2	49.4	52.0	0.27	0.37	0	0	33.5	65.5	0.43	0.80
cfo1	48.8	51.4	0.26	0.41	0	-0.07	22.7	77.7	0.54	2.40

and less distorted environments for Fe ions on the B-sites for the *cfo2* powder, where the number of Co^{2+} ions on the A-sites is lower. Similarly, Goya et al. [14] reported that the occupation of the octahedral sites by Cu^{2+} ions led to crystal distortion also in $CuFe_2O_4$ nanoparticles. The Fe cation inversion degree is lower for the *cfo3* powder than for the *cfo1* one, although further disorder, due to mechanical milling, could be expected for the *cfo3* one. For this sample, the additional TA performed after milling could be the origin of reduction of Co^{2+} population on the A-sites.

Different cation occupancy on the A- and the B-sites of the samples of equal crystallite size (36 nm, *cfo1* and *cfo3*) shows the predominant dependency of the samples on the thermal history [15] rather than particle size.

Based on the results of the ME technique, we can conclude that $CoFe_2O_4$ nanopowders used to consolidate the target for deposition of the CFO2 film seem to be structurally less distorted. Opposite conclusions can be made about the $CoFe_2O_4$ nanopowders used as a target to grow the CFO1 film.

From the full width at half maximum of the diffraction peak (β) and its angular position, it is possible to build a Williamson–Hall (W–H) plot. Using (111), (222) and (333) Bragg peaks we plotted W–H graphs (Fig. 3). The slope of the linear fit gives into account the strain present in the sample. The film with the largest strain is the CFO1 one, while the film with the smallest strain is CFO2 (see Table 1). The CFO3 film revealed a slope in the W–H plot with an intermediate value, in agreement with the corresponding results from Mössbauer analysis of target powder.

In such a way, we state the fact of a correlation between the structure of powder and films: structurally more distorted target originates more tension at the film surface. Nevertheless, this statement could fail if the processing conditions are not thoroughly kept the same.

We believe that the observed correlation is due to three-dimensional islands (of target's material) consisting of some cobalt ferrite cells being extracted during the deposition procedure, preserving some structural features of the material from the target.

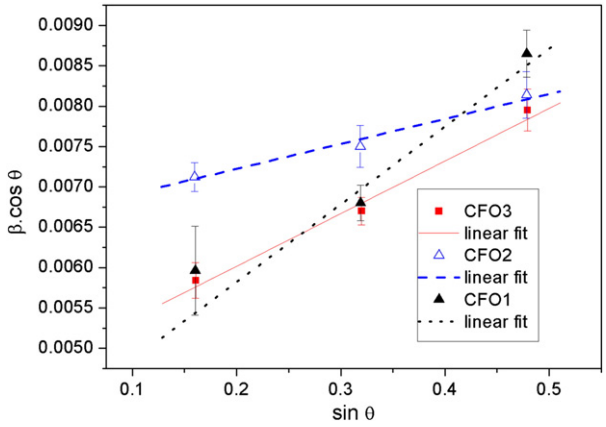

Fig. 3. Williamson–Hall graphs obtained from the X-ray reflections of the XRD patterns of the cobalt ferrite films (on the base of (111), (222) and (333) planes).

Fig. 4a shows the XANES signals of CFO1 and CFO2 films as well as the signal of *cfo2* powder taken as a reference. The pre-edge structure, observed in the spectra, is characteristic of Fe in a distorted octahedrally coordinated environment that arises from electronic $1s \rightarrow 3d$ quadrupole and $1s \rightarrow 3d/4p$ hybridized orbital dipole transitions. It can be observed, that there is a shift to higher energies in the Fe K-edge for *cfo2*. This fact means that in the nanopowders the photoelectron has higher binding energies. This could be attributable to empty states created below the metallic Fe Fermi level, as it could be, for example, the situation for trapped electrons due to oxygen vacancies. During the film growth a partial reduction of the oxygen vacancies is expected.

The pre-peak amplitude is higher in the CFO1 film than in the CFO2 one, indicating an increase of the degree of orbital *p–d* mixing that could indicate that the central Fe atoms occupy a more non-centrosymmetric environment [16]. The white line amplitude is smaller for the CFO1 film than for the CFO2 one. This could indicate the presence of Fe 3+ with coordination lower in the former than in the latter one. This fact means that the crystal distortion observed by ME could be originated not only by cation inversion but by oxygen vacancy as well. These results explicitly demonstrate that using more perfect targets leads to fabrication of structurally less distorted films.

One of the important points to pay attention is the chemical homogeneity of cobalt ferrite films. In such a sense, in Fig. 4b we show GIXRF measurement of the CFO1 film, namely, the intensity of Fe and Co K_α lines as a function of the incident angle. Both intensities have the same behavior which is an indication that quantitative proportion between Fe and Co is uniform with depth in the film.

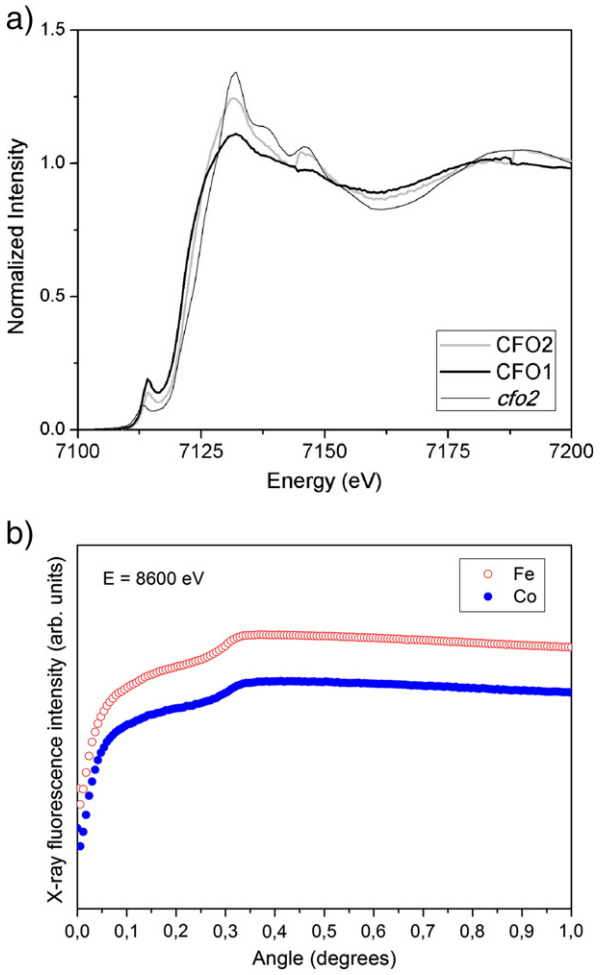

Fig. 4. a. Fe K-edge XANES spectra using an incident angle of 0.38° of CFO1 and CFO2 films and *cfo2* powder (latter, in transmission mode). b. GIXRF: intensity of Fe and Co K_α lines as a function of the incident angle for the CFO1 film.

In order to get more proofs about structural dependence between the film and the target that we have observed by XRD, XANES and ME, we decided to extract additional information about our films indirectly (from a magnetic point of view). It was not a simple task for monolayer films, so we found a manner to do it implementing bilayer systems. Particularly, it was able due to the presence of the so called EB effect in these bilayers. When a ferromagnet (FM) is in contact with an antiferromagnet (AFM), a shift of the hysteresis loop along the magnetic-field axis can occur being called exchange bias. Also this effect was observed in FM/HFi (hard ferrimagnetic) bilayers [17]. Usually, this shift is observed after cooling the entire system in an external magnetic field below the Néel temperature of the AFM or HFi.

Additionally, we deposited a Fe layer (about 30 nm) on each cobalt ferrite film. The Fe layer was passivated with a tiny cap layer of TiO_2. That was performed also by the PLD technique at 400 °C. The new system (now FM/HFi bilayer) was subjected to M vs H measurements—first, at 300 K, and later, at 20 K after cooling the system with an applied magnetic field of 3 T. For comparison purposes, an M vs H loop at 20 K without field cooling was also measured. All magnetic loops are shown in Fig. 5a. As it can be seen at low temperature curves, the magnetic response of the system reflects the magnetically uncoupled state (as expected for manifestation of EB [17]) of the bilayer system, where EB effect arises between FM and HFi materials. The magnitude of exchange bias field, H_{EB}, is quantified as the semi-sum of coercive fields. From 20 K-hysteresis loops after field cooling we obtained the following results: $H_{EB} = 41.8$ kA/m corresponds to the bilayer with the CFO2 film, $H_{EB} = 51.7$ kA/m corresponds to the bilayer with the CFO1 film while the sample with CFO3 revealed $H_{EB} = 47.1$ kA/m. In other words, the maximum value of the EB field reveals the bilayer where the cobalt ferrite film is more defective. Meanwhile the bilayer, where the cobalt ferrite film is less defective, reveals the minimum value of the EB field (Fig. 5b). This is in agreement with the results of Nowak et al. who demonstrated, both experimentally and by Monte Carlo simulations, a strong dependence of the EB field on the concentration of crystallographic defects in the volume part of the pinning layer [18]. Also, these results are compatible with our XRD, XANES and Mössbauer studies and reinforce the idea about structural correlation between the target and the film.

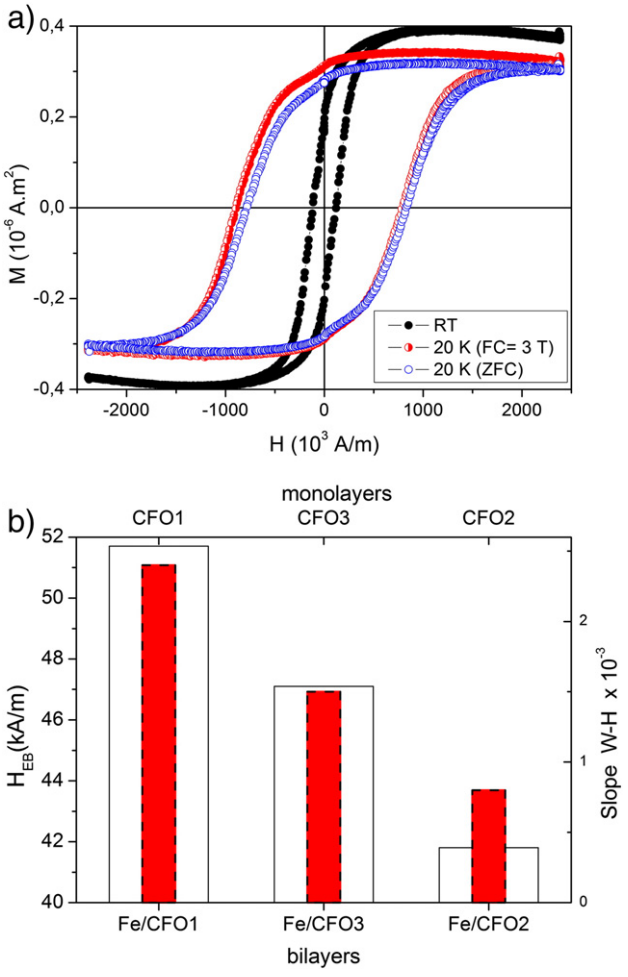

Fig. 5. a. CFO1 film: hysteresis loops. b. Exchange bias field values of bilayers (empty rectangular column); values of the slope of the Williamson–Hall graph of cobalt ferrite monolayers taken from Table 1 (full rectangular column).

4. Conclusions

We prepared a series of cobalt ferrite films under the same deposition conditions by PLD using targets of $CoFe_2O_4$ nanopowders which were chemically synthesized under distinct conditions in order to induce a different degree of crystal distortion. Based on the results of ^{57}Fe ME, XRD and XANES techniques, we registered direct evidences of the structural target–film correlation. These evidences are supported indirectly by magnetic property observation (strength of exchange bias field) which involved an additional deposition of a magnetically soft layer. We have noted that the thermal history of the target material is crucial for inducing strain in the films. Our results explicitly demonstrate that the cobalt ferrite thin films' quality depends on the degree of the quality of the precursor material when the PLD technique is involved. It could help tuning the magnetic properties of films when particular features are highly desirable for technological applications.

Acknowledgments

The authors thank Dr. R. Martínez García for helping in the chemical synthesis of the nanopowders and Dr. U. Wolff for VSM facilities. We appreciate the support by LNLS, Campinas—SP, Brazil.

References

[1] M. Gomi, H. Toyoshima, Heteroepitaxial growth of α-Fe_2O_3 thin films on (111) GGG, Jpn. J. Appl. Phys. 35 (1996) L544.
[2] T. Tepper, F. Ilievski, C.A. Ross, T.R. Zaman, R.J. Ram, S.Y. Sung, B.J.H. Stadler, Magneto-optical properties of iron oxide films, J. Appl. Phys. 93 (2003) 6948.
[3] R. Eason, Pulsed Laser Deposition of Thin Films: Applications-Led Growth of Functional Materials, Wiley-Interscience, Hoboken, NJ, 2007.
[4] J. Shen, Zheng Gai, J. Kirschner, Growth and magnetism of metallic thin films and multilayers by pulsed-laser deposition, Surf. Sci. Rep. 52 (2004) 163.
[5] R. Sayed Hassan, N. Viart, C. Ulhaq-Bouillet, J.L. Loison, G. Versini, J.P. Vola, O. Crégut, G. Pourroy, D. Muller, D. Chateigner, Structural properties of cobalt ferrite thin films deposited by pulsed laser deposition: effect of the reactive atmosphere, Thin Solid Films 515 (2007) 2943.
[6] P.D. Thang, G. Rijnders, D.H.A. Blank, Stress-induced magnetic anisotropy of $CoFe_2O_4$ thin films using pulsed laser deposition, J. Magn. Magn. Mater. 310 (2007) 2621.
[7] C. Araújo, B.G. Almeida, M. Aguiar, J.A. Mendes, Structural and magnetic properties of $CoFe_2O_4$ thin films deposited by laser ablation on Si (001) substrates, Vacuum 82 (2008) 1437.
[8] H. Yanagihara, K. Uwabo, M. Minagawa, Eiji Kita, Noriyuki Hirota, Perpendicular magnetic anisotropy in CoFe2O4 (001) films epitaxially grown on MgO (001), J. Appl. Phys. 109 (2011) 07C122.
[9] Devajyoti Mukherjee, Tara Dhakal, Manh-Huong Phan, Hariharan Srikanth, Pritish Mukherjee, Sarath Witanachchi, Role of crystal orientation on the magnetic properties of $CoFe_2O_4$ thin films grown on Si (1 0 0) and Al_2O_3 (0 0 0 1) substrates using pulsed laser deposition, Physica B 406 (2011) 2663.
[10] C.E. Rodríguez Torres, F. Golmar, M. Ziese, P. Esquinazi, S.P. Heluani, Evidence of defect-induced ferromagnetism in $ZnFe_2O_4$ thin films, Phys. Rev. B 84 (2011) 064404.
[11] A. Yang, Z. Chem, Sh.M. Islam, C. Vittoria, V.G. Harris, Cation engineering of Cu-ferrite films deposited by alternating target laser ablation deposition, J. Appl. Phys. 103 (2008) 07E509.
[12] A. Medina-Boudri, D. Bueno-Baqués, L. Fuentes-Cobas, M. Miki-Yoshida, Study of reversible and irreversible magnetization processes of coprecipitated cobalt ferrite, J. Appl. Phys. 87 (2000) 6235.
[13] A. Goldman, Modern Ferrite Technology, Van Nostrand Reinhold, New York, 1990.
[14] G.F. Goya, H.R. Rechenberg, J.Z. Jiang, Magnetic irreversibility and relaxation in $CuFe_2O_4$ nanoparticles, J. Magn. Magn. Mater. 218 (2000) 221.
[15] J.P. Chen, K.J. Klabunde, G.C. Hadjipanayis, E. Delvin, A. Kostikas, Phys. Rev. B 54 (1996) 92;

J.P. Chen, K.J. Klabunde, G.C. Hadjipanayis, E. Delvin, A. Kostikas, Size-dependent magnetic properties of $MnFe_2O_4$ fine particles synthesized by coprecipitation, Phys. Rev. B 54 (1996) 9288.
[16] Frank de Groot, Gyorgy Vankó, Pieter Glatzel, The 1s X-ray absorption pre-edge structures in transition metal oxides, J. Phys. Condens. Matter 21 (2009) 104207.
[17] F. Radu, R. Abrudan, I. Radu, D. Schmitz, H. Zabel, Perpendicular exchange bias in ferrimagnetic spin valves, Nat. Commun. 3 (2012) 715.
[18] U. Nowak, K.D. Usadel, J. Keller, P. Miltenyi, B. Beschoten, G. Guntherodt, Domain state model for exchange bias. I. Theory, Phys. Rev. B 66 (2002) 014430.